J Appl Physiol 117: 1502–1513, 2014.
First published October 16, 2014; doi:10.1152/japplphysiol.00713.2014.

Bronchoprotective effect of simulated deep inspirations in tracheal smooth muscle

Christopher D. Pascoe,[1,6] Graham M. Donovan,[2] Ynuk Bossé,[5] Chun Y. Seow,[3,6] and Peter D. Paré[4,6]

[1]*Department of Medicine, University of British Columbia, Vancouver, British Columbia, Canada;* [2]*Department of Mathematics, University of Auckland, Auckland, New Zealand;* [3]*Department of Pathology and Laboratory Medicine, University of British Columbia, Vancouver, British Columbia, Canada;* [4]*Department of Medicine, Respiratory Division, University of British Columbia, Vancouver, British Columbia, Canada;* [5]*Institut Universitaire de Cardiologie et de Pneumologie de Québec, Université Laval, Québec, Canada; and* [6]*Center for Heart Lung Innovation, St. Paul's Hospital, Vancouver, British Columbia, Canada*

Submitted 6 August 2014; accepted in final form 8 October 2014

Pascoe CD, Donovan GM, Bossé Y, Seow CY, Paré PD. Bronchoprotective effect of simulated deep inspirations in tracheal smooth muscle. *J Appl Physiol* 117: 1502–1513, 2014. First published October 16, 2014; doi:10.1152/japplphysiol.00713.2014.—Deep inspirations (DIs) taken before an inhaled challenge with a spasmogen limit airway responsiveness in nonasthmatic subjects. This phenomenon is called bronchoprotection and is severely impaired in asthmatic subjects. The ability of DIs to prevent a decrease in forced expiratory volume in 1 s (FEV_1) was initially attributed to inhibition of airway narrowing. However, DIs taken before methacholine challenge limit airway responsiveness only when a test of lung function requiring a DI is used (FEV_1). Therefore, it has been suggested that prior DIs enhance the compliance of the airways or airway smooth muscle (ASM). This would increase the strain the airway wall undergoes during the subsequent DI, which is part of the FEV_1 maneuver. To investigate this phenomenon, we used ovine tracheal smooth muscle strips that were subjected to shortening elicited by acetylcholine with or without prior strain mimicking two DIs. The compliance of the shortened strip was then measured in response to a stress mimicking one DI. Our results show that the presence of "DIs" before acetylcholine-induced shortening resulted in 11% greater relengthening in response to the third DI, compared with the prior DIs. This effect, although small, is shown to be potentially important for the reopening of closed airways. The effect of prior DIs was abolished by the adaptation of ASM to either shorter or longer lengths or to a low baseline tone. These results suggest that DIs confer bronchoprotection because they increase the compliance of ASM, which, consequently, promotes greater strain from subsequent DI and fosters the reopening of closed airways.

asthma; airway hyperresponsiveness; muscle mechanics; mathematical modeling

TWO OF THE CARDINAL FEATURES of asthma are the failure of deep inspirations (DIs) to dilate constricted airways (20, 42) and the inability of DIs taken before methacholine challenge to attenuate subsequent airway responsiveness (26). The former of these two phenomena is known as DI-induced bronchodilation, and the latter is known as DI-induced bronchoprotection. Malmberg et al. (36) first showed the bronchoprotective effect of DIs in nonasthmatic subjects, whereby two DIs taken up to 10 min before the administration of methacholine attenuated the decrease in forced expiratory volume in 1 s (FEV_1). This phenomenon later became known as the bronchoprotective effect of DIs (26) and was shown to be absent in asthmatic subjects (54). It has also been shown that bronchoprotection has a larger effect than does the bronchodilation effect of DIs (51), and that the former is more likely to be associated with airway hyperresponsiveness (AHR) (52). Yet the bronchoprotective effect of DIs is only seen when airway narrowing is assessed after challenge using a test that requires a DI (such as FEV_1) (11, 15). When airway narrowing is assessed using airway conductance or maximal flows on partial flow volume curves (8), there is no beneficial effect of prior DIs and no differences between asthmatic and normal subjects. These results imply that the prior DIs act to make the airways more responsive to the bronchodilator effect of subsequent DIs.

Airway smooth muscle (ASM) displays remarkable plasticity and can adapt to a wide range of lengths while maintaining its ability to develop force and shorten (7, 47, 59). This is known as length adaptation and has been postulated to be a mechanism contributing to AHR in asthma (4). ASM can also adapt to basal tone induced by contractile agonists in a phenomenon known as force adaptation (5, 43). Force adaptation could stiffen the ASM and the airway wall and act to prevent stretching of the ASM layer, thereby limiting bronchoprotection. Length adaptation is also known to stiffen ASM (21, 37, 59) and could act alone or in concert with force adaptation to inhibit the beneficial effects of DIs.

We hypothesized that simulated DIs taken before ASM shortening would increase the compliance of ASM to a subsequent DI, and that adaptation to shorter lengths or induction of force adaptation would lead to inhibition of this bronchoprotective effect. Our data indicate that prior DIs do not affect the amount of shortening induced by acetylcholine (ACh) but modestly increase the compliance of ASM to a subsequent DI. We also show that length adaptation and force adaptation can inhibit the increased compliance caused by prior DIs. Together, our data suggest that increased ASM compliance due to prior DIs contributes to the bronchoprotective effect of DIs in nonasthmatic airways.

MATERIALS AND METHODS

Muscle preparation. Sheep tracheas used in these experiments were obtained from a local abattoir. The use of the tissue was approved by the Committees on Animal Care and Biosafety of the University of British Columbia. Tracheas were removed soon after the animals were killed and put into Krebs solution (pH 7.4; 118 mM NaCl, 4 mM KCl, 1.2 mM NaH_2PO_4, 22.5 mM $NaHCO_3$, 2 mM $MgSO_4$, 2 mM $CaCl_2$, and 2 g/l dextrose). On arrival at the laboratory, tracheas were cleaned

Address for reprint requests and other correspondence: C. D. Pascoe, Center for Heart Lung Innovation, UBC, 1081 Burrard St., Rm. 166, Vancouver, BC, Canada V6Z 1Y6 (e-mail: chris.pascoe@hli.ubc.ca).

of blood, fat, and loose connective tissue and stored in Krebs solution at 4°C until further processed. ASM strips for experiments were dissected from ~2-cm-long tracheal segments. Two small incisions were made in the epithelium when the relaxed tracheal smooth muscle bundles were still connecting the C-shaped cartilage rings, and the distance between the incisions was measured. These were used as landmarks to preserve the in situ length of ASM during the dissection. The tracheal rings were then cut open, unfolded, and secured at a length adjusted so that the distance between the two epithelial incisions was the same as measured in the closed rings. Cartilage, adventitial connective tissue, and the epithelial layer were dissected away from the tracheal smooth muscle layer, and muscle strips (~7 mm long, 1 mm wide, and 0.3 mm thick) were isolated without cutting the anchoring points on the cartilage at both ends. An aluminum foil clip was then attached on both ends of the muscle strips, and the distance between the clips was measured. The strips were then mounted vertically in an organ bath. The bottom clip was attached to a stationary hook, while the upper clip was attached to a hook connected to the lever arm of a servo-controlled force-length transducer by a surgical thread (size 6). The distance between the clips measured during the dissection was used to adjust the length of the ASM strip to the length that it was in situ. This length is hereafter called L_{ref}. The organ bath was filled with Krebs solution that had been preheated to 37°C and aerated with a gas mixture containing 95% O_2 and 5% CO_2. The temperature of the bath was also maintained by circulating 37°C water through a jacket that surrounded the organ bath.

Equilibration period. ASM strips were subjected to an equilibration period before the start of the experiments. During equilibration, the baseline tone of the ASM strips was monitored. Once the baseline tone decreased to ~2–3 mN, the strips were activated every 5 min with a 9-s electrical field stimulation (EFS) (60 Hz, 12 V). Krebs solution was replaced every 5 min following EFS with warmed (37°C), aerated Krebs solution. The equilibration was completed when a plateau in isometric force was reached (i.e., after which there was no further increase in force in response to subsequent EFS). The force produced by EFS at that time was called F_{max}. Therefore, F_{max} was the force generated by the ASM in response to EFS at L_{ref} after a stable plateau was achieved. The equilibration period took ~1 h.

Calculation of force oscillations [adapted from Pascoe et al. (44)]. The stress oscillations imposed on the ASM strips in this study simulated the tension oscillations experienced by the wall of a fourth-generation airway during transpulmonary pressure excursions of different magnitude; e.g., 3 cmH_2O to mimic tidal breathing and 25 cmH_2O to mimic a DI from functional residual capacity to total lung capacity (TLC). The changes in wall tension caused by pressure oscillation excursions were calculated based on the Laplace relationship (tension = pressure × radius), assuming that the airways resemble a thin-walled cylinder (an appropriate assumption since the wall thickness/airway luminal diameter ratio is ~1/22 in nonasthmatic airways of the fourth generation) (24, 27). Since the airway wall is also strained during these swings in transpulmonary pressure, the calculated change in wall tension also has to take into account the change in radius (at the middle of the ASM layer). Equations developed by Lambert and coworkers (29) and morphological data for a fourth-generation airway (24, 27, 60) were used to make this adjustment. The magnitude of the tension oscillations was the same for every ASM strip, but the magnitude of the force oscillations depended on the width of the ASM strip. Since the ASM is arranged circumferentially around the airways, this width represented the portion of the airway length that would be studied. We estimated the width of the ASM strips by assuming the ASM generates a stress of 100 kPa in response to EFS following the equilibration period, and that the thickness of the ASM strips was ~0.3 mm. The value of force (in mN) was then used to calculate the width of the ASM strips. Knowing the length of the airway wall that would be covered in situ by this estimated width and the changes in wall tension occurring during breathing maneuvers, we were then able to calculate the force oscillations (in mN) that needed to be imposed on the tracheal strips to simulate the stress to which the ASM is subjected in vivo. This approach has been used in our laboratory's two previous studies and provides force oscillations that result in physiological strains in relaxed conditions (43, 44). A similar approach for calculating load on ASM during a DI has been previously used by others in ovine tracheal strips (41).

Bronchoprotection protocol. Following equilibration of the tissue, we examined the effect of prior length perturbations that mimic DIs on subsequent shortening of the muscle and its response to a third force-controlled DI maneuver. Specifically, the interventions began with two stretches of 25% L_{ref}, which were applied to mimic two DIs to TLC. The stretches were applied over 5 s each. The control protocol was identical, except that no simulated DIs were applied. The order of the control or experimental protocols was randomly assigned. Ten seconds after the DIs (or at the same time without DIs), the lever was switched to force control, and the tissue was shortened with ACh (1 μM) against an isotonic load equivalent to 15% of F_{max}. The muscle was allowed to shorten to a plateau value for 60 s, after which a third quick (over 0.5 s) DI-like stretch was applied (see Fig. 1). This third DI stretch was achieved by applying a force perturbation calculated to be equivalent to a DI achieved with an inspiratory pressure of 25 or 50 cmH_2O. Calculations of the amplitude of the stress perturbation needed to mimic in vivo pressure changes of 25 and 50 cmH_2O were done in the same manner as described earlier. Following 100 s of recording, the ASM was washed three times with Krebs solution to remove the ACh and allowed to return to L_{ref} by itself. The tissue was then left to recover for 30 min. During this recovery time, there was no EFS stimulation, and the tissue was washed with Krebs every 5 min. Following the recovery period, the tissue was stimulated once again with EFS until a stable plateau was reached. Following reequilibration, the tissue was subjected to the alternate protocol. For both control and experimental protocols, we measured the amount of maximal shortening before the third DI stretch was applied, the peak relengthening (strain) in response to the third DI stretch, and the rate of reshortening ($T_{1/2}$ or time taken to reshorten to one-half of the maximal reshortening) following the stretch.

This standard bronchoprotection protocol was applied to ASM tracheal strips under four different conditions. *1*) ASM was kept at L_{ref}, and two different amplitudes of stress oscillations were used for the third DI stretch. One mimicked a normal airway transmural pressure achieved during a typical inspiration to TLC (25 cmH_2O), while the other amplitude mimicked a supramaximal pressure oscillation (50 cmH_2O). *2*) Tissue was shortened by 30% and allowed to length adapt for 1 h. During the first 30 min, the tissue was allowed to equilibrate with no stimulation, and, for the subsequent 30 min, it was stimulated once every 5 min until a stable plateau in force was reached. *3*) Tissue was stretched by 30% and allowed to length adapt in the same manner. *4*) Tissue was exposed to a low level of ACh stimulation ($\sim 5 \times 10^{-8}$ M) and stimulated repeatedly at 5-min intervals with EFS to induce force adaptation. Once force adaptation was induced [in a similar manner to Bosse et. al. (5)], the bronchoprotective protocol was applied. In the case of force adaptation, the two prior DIs were force-controlled perturbations (25 cmH_2O) instead of length oscillations. This is because, with increased tone, a 25% length perturbation would require an applied stress greater than would be expected in vivo (44).

Calculation of resistance change due to prior DIs. A simple model of a single airway with a radius of 1 mm was used to calculate the change in airflow resistance that would result from the prior DI's effect on the length changes induced by the subsequent FEV_1-like DI. It was assumed that the change in length of the ASM strip ex vivo was proportional to the change in circumference of the airway lumen. Airflow resistance (R) was calculated using the Poiseuille equation: $R = 8\eta L/\pi r^4$, where η is the viscosity of the air, L is the length of the airway, and r is the radius of the airway. Assuming that, between the

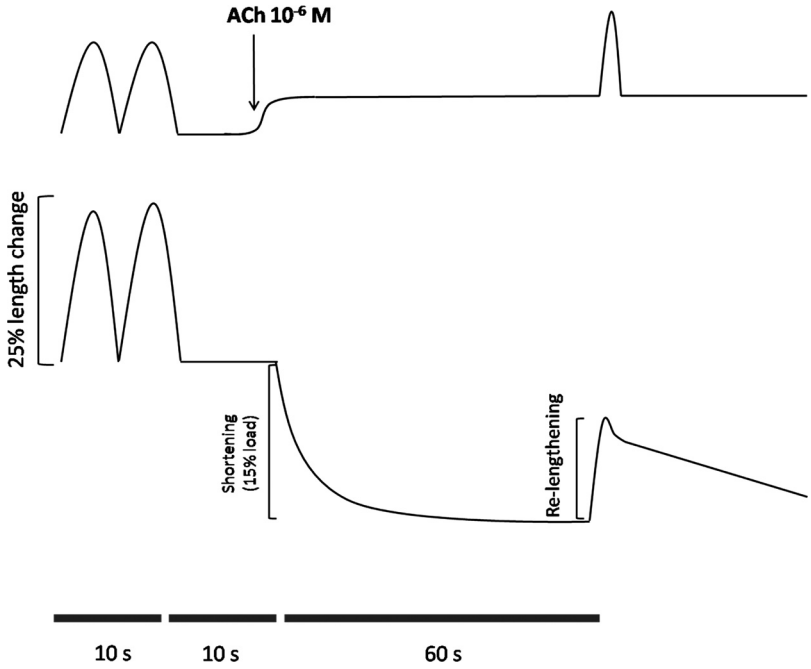

Fig. 1. Schematic of bronchoprotection protocol. *Top*: force trace. *Bottom*: length trace.

control and prior DI protocol, the only variable that changed was the radius, we were able to calculate the change in resistance due to the prior DIs. For example, the viscosity of air and length of the airway were both set to 1, so that the equation simplified to $R = 8/\pi r^4$. With the control radius following activation set to 1, the resistance in this airway was 2.55 $cmH_2O \cdot l^{-1} \cdot s$. Changing the radius in the prior DI setting by the same percentage as the increase in length in the ASM strips yielded the resistance in each of the test conditions. This calculation was done for all the tissue conditions (L_{ref}, 70% L_{ref}, 130% L_{ref}, and force adapted) and expressed as percent change from control.

Computational modeling. To examine the possible role of airway reopening, a computational model of the human lung was employed to test the effect of bronchoprotection. The airway tree geometry was taken from a previously reported model (56), and each airway in that tree has dynamics similar to those described in previous reports (16, 17, 46) with explicit representations of both airway wall compliance and parenchymal tethering forces based on experimental data, as well as ASM length-tension relationships obtained from the data in this paper. We assumed an initially normally distributed range of ASM tension, and the degree of constriction is adjusted until the respiratory impedance reaches a prescribed level (to simulate agonist challenge). We assume that this "challenged" lung then has a bimodal distribution of radii, with closed and open populations, which can exist because of the bistability of the airway radius in terms of ASM tension in the small airways (1). [Note that the model does not address the formation of this bimodal distribution, but rather takes it as a starting point on the basis of other work (2, 57).] To simulate the third DI maneuver, ASM force-length loops are fit to the experimental data collected in this study, both for the control and prior DI situations. The difference in these force-length loops were the only thing that separated the control and prior DI cases; the challenged lung is assumed to be identical in both cases. A 30-cmH_2O DI is imposed on the challenged lung, driving reopening of some closed airways, with airway opening being determined by the force-length relationships. For complete model details please see the APPENDIX.

Statistical analysis. Maximal shortening, peak relengthening, and $T_{1/2}$ were normalized to L_{ref} for each strip of muscle. Data are means ± SE. Analysis of time course of reshortening was done using a repeated-measures two-way ANOVA. Analysis of maximal shortening, peak relengthening, and $T_{1/2}$ was done using a paired *t*-test. Analysis of the change in airflow resistance was done using a paired Student's *t*-test. All graphs and analysis were done using Prism 5 (GraphPad Software, San Diego, CA). A $P < 0.05$ was considered significant.

RESULTS

Effect of prior DIs at L_{ref}. All tissues were shortened against a 15% F_{max} load with 1 μM ACh. In tissues where the third DI was of an amplitude equivalent to 25 cmH_2O, tissues without prior DIs (control) shortened by 37.0 ± 6.0% vs. tissues with prior DIs that shortened by 35.3 ± 6.0% (Fig. 2*A*, $P < 0.05$). When the third DI was of an amplitude equivalent to 50 cmH_2O, tissues without prior DIs (control) shortened by 37.5 ± 4.1%, which was similar to tissues with prior DIs that shortened by 38.6 ± 3.4% (Fig. 2*B*, $P > 0.05$). The peak strain in response to both amplitudes of DI is shown in Fig. 3. In both cases, prior DIs enhanced the relengthening of the tissue in response to the third DI maneuver. The 25-cmH_2O DI strained the tissue by 10.1 ± 1.3% in the control intervention and by 11.3 ± 1.6% with prior DI (Fig. 3, *A* and *B*, $P = 0.016$). Figure 3*A* also shows the time course of reshortening following the DI. The two curves are significantly different ($P < 0.0001$) by repeated-measures two-way ANOVA. The $T_{1/2}$ is not significantly different between conditions (8.1 ± 1.1 s prior DI vs. 7.9 ± 1.0 s control, $P > 0.05$). The 50-cmH_2O DI strained the tissue by 18.0 ± 1.2% in the control intervention and by 19.2 ± 1.4% in the prior DI intervention (Fig. 3, *C* and *D*, $P = 0.001$). Figure 3*C* shows the time course of reshortening following the DI. The two curves are significantly different ($P < 0.0001$) by repeated-measures two-way ANOVA. The $T_{1/2}$ was significantly different between control (5.8 ± 2.4 s) and prior DI (6.4 ± 2.5 s) interventions ($P < 0.002$).

Effect of length adaptation on bronchoprotection. Tissues adapted to shorter (70% L_{ref}) or longer (130% L_{ref}) lengths were considered adapted when force in response to EFS plateaued to a new F_{max}. Tissues adapted to 70% L_{ref} showed

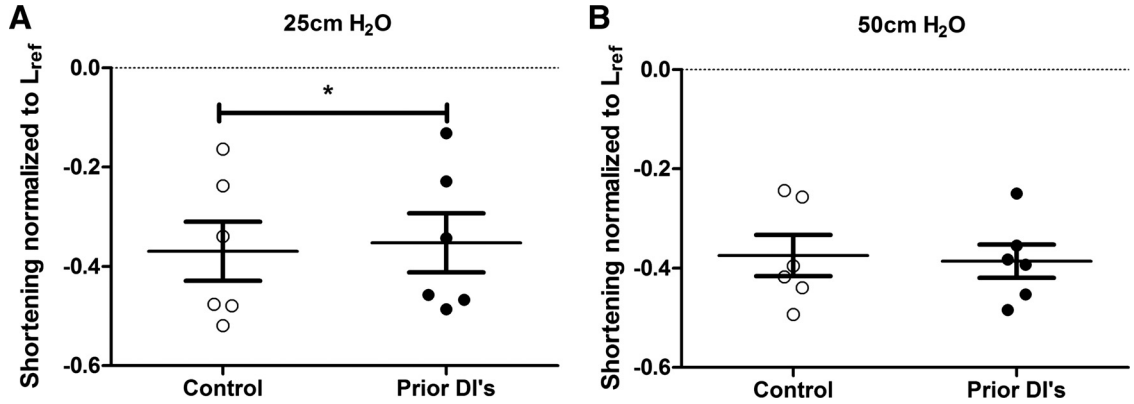

Fig. 2. Maximal preforce controlled deep inspiration (DI) shortening induced by 1 μM ACh in strips that were subsequently subjected to a third DI of amplitude equivalent to either 25 cmH_2O (*A*) or 50 cmH_2O (*B*). L_{ref}, reference length. *$P < 0.05$ with paired *t*-test.

similar levels of shortening between the control and prior DI conditions (14.1 ± 0.89 vs. 13.5 ± 0.96%, $P > 0.05$); see Fig. 4*A*. For tissues adapted at 130% L_{ref}, shortening was also similar at 59.8 ± 4.0% in the control condition and 58.9 ± 3.6% in the prior DI condition ($P > 0.05$, Fig. 4*B*). There appeared to be no effect of prior DIs on shortening when the data for all tissues (70% L_{ref}, 130% L_{ref}, and L_{ref}) are combined (Fig. 4*C*, $P > 0.05$).

For tissues adapted to 70% L_{ref}, prior DIs had no effect on the subsequent strain of the third DI maneuver (8.8 ± 0.011 vs. 8.9 ± 0.011%, $P > 0.05$) (Fig. 5*B*) or the reshortening in response to the third DI maneuver (Fig. 5*A*, $P > 0.05$). Prior DIs did not affect the rate of reshortening ($T_{1/2}$) following the stretch (11.5 ± 1.9 vs. 11.4 ± 1.6 s, $P > 0.05$). For tissues adapted to 130% L_{ref}, prior DIs significantly increased the length change during and after the subsequent DI, as measured by a repeated-measures two-way ANOVA (Fig. 5*C*, $P = 0.002$). However, the peak strain induced by the third DI maneuver (Fig. 5*D*) in the prior DI protocol was not significantly greater than for the control condition (10.9 ± 0.58 vs. 11.4 ± 0.50%, $P > 0.05$). The $T_{1/2}$ was also not significantly different between the control condition and prior DI condition (11.2 ± 1.3 vs. 11.1 ± 1.7 s, $P > 0.05$).

Force adaptation and bronchoprotection. Force adaptation was induced using 50 nM ACh and was measured and identified as an increase in EFS-induced force that increased to a new plateau following three to five EFS stimulations at 5-min intervals (Fig. 6*A*). The degree of force adaptation in the two

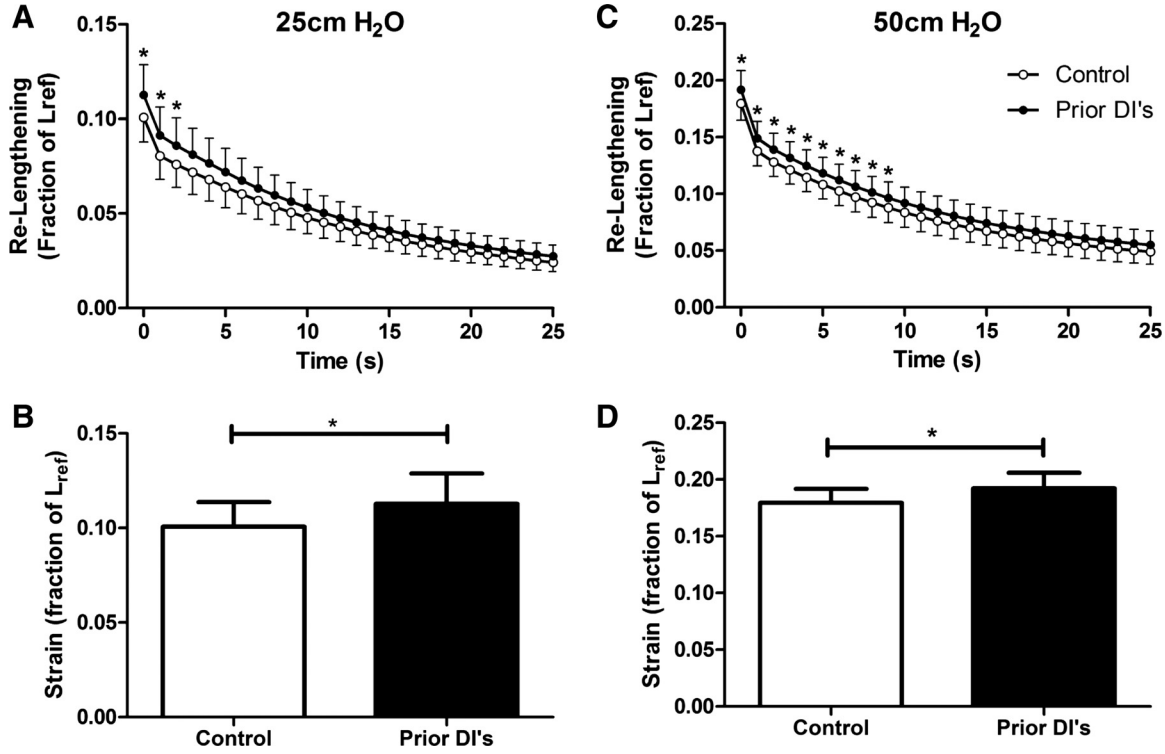

Fig. 3. Time course of reshortening following third DI maneuver equivalent to 25-cmH_2O (*A*) or 50-cmH_2O (*C*) pressure is shown. Peak strain of tissue in response to a force controlled DI of 25 cmH_2O (*B*) or 50 cmH_2O (*D*) is shown. Values are means ± SE. *$P < 0.05$ by repeated-measures two-way ANOVA (*A* and *C*) or paired *t*-test (*B* and *D*).

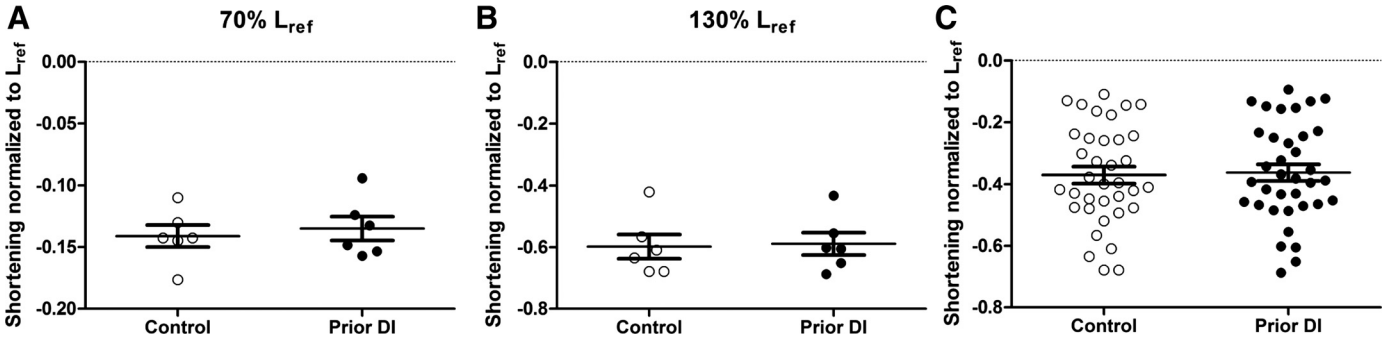

Fig. 4. Maximal preforce controlled DI shortening induced by 1 μM ACh in strips length-adapted to 70% L_{ref} (*A*) or 130% L_{ref} (*B*). *C*: comparison of shortening in all conditions pooled. The length is normalized to L_{ref}, but the shortening is relative to the adapted length.

protocols was not significantly different ($P > 0.05$). The shortening induced by 1 μM ACh was also not significantly different between the two conditions, with the control tissues shortening by an average of 34.1 ± 3.7% and tissues subjected to prior DI shortening by 32.7 ± 4.0% (Fig. 6*C*, $P > 0.05$). In the presence of force adaptation, prior DIs did not affect the magnitude of the strain induced by the third DI maneuver, nor did they affect the subsequent reshortening (Fig. 6, *B* and *D*, $P > 0.05$). The peak strain induced by the third DI maneuver was 11.0 ± 1.4% for the control and 11.2 ± 0.92% for the prior DI conditions, respectively. Again, $T_{1/2}$ was not significantly different between the two conditions (4.3 ± 2.0 vs. 4.4 ± 1.3 s, $P > 0.05$).

Modeling the change in airflow resistance. To understand the potential functional consequence of the increased strain induced by a third DI maneuver following prior DIs, as well as the effect length and force adaptation had on blunting this increase, we modeled the change in resistance to airflow in a single airway. The change in resistance to airflow can be seen in Table 1. When the ASM tissue was at L_{ref}, the decrease in airflow resistance elicited by the DI on an ACh-constricted airway was 33.3 ± 4.73% greater with prior DIs than without prior DIs. This change in resistance was statistically significant (Fig. 7, $P < 0.001$). When the tissues were adapted to a shorter length, the change in airflow resistance of an airway was not different from the control condition (1.48 ± 13.7% increase, $P > 0.05$). Additionally, adaptation to longer lengths caused the prior DIs to have a nonsignificant effect on the reduction in airflow resistance in response to the third DI maneuver (11.7 ± 12.6% decrease over control, $P > 0.05$). Induction of force adaptation also ablated the change in airflow resistance caused by the prior DIs compared with the control (no prior DIs) condition (11.9 ± 35.6% increase, $P > 0.05$). These values can be found in Table 1.

Modeling the effect at the organ level. Using the computational model, we found that the differential ASM response to prior DIs during the third DI maneuver, although modest at the tissue level, can drive additional airway reopening at the organ level. Furthermore, we find that this additional reopening may be enough to account for significant differences in lung function post-DI and hence account for the bronchoprotective effect of prior DIs.

In the challenged lung, we assume that there is a bimodal distribution of airway radii, with a closed population and an open population. Specifically, the model challenged lung has 9,305 "closed" airways out of 30,941 total (30.1% closed). The

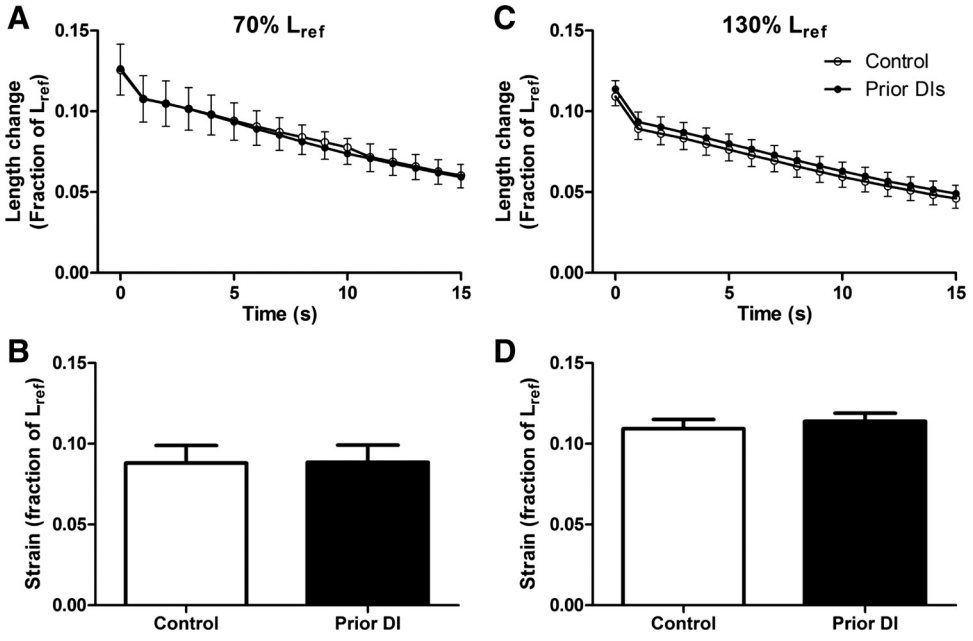

Fig. 5. Time course of reshortening following third DI maneuver in tissues adapted to lengths of 70% L_{ref} (*A*) or 130% L_{ref} (*C*) is shown. Peak strain of tissue in response to a force controlled DI in tissue adapted to lengths of 70% L_{ref} (*B*) or 130% L_{ref} (*D*) is shown. Values are means ± SE.

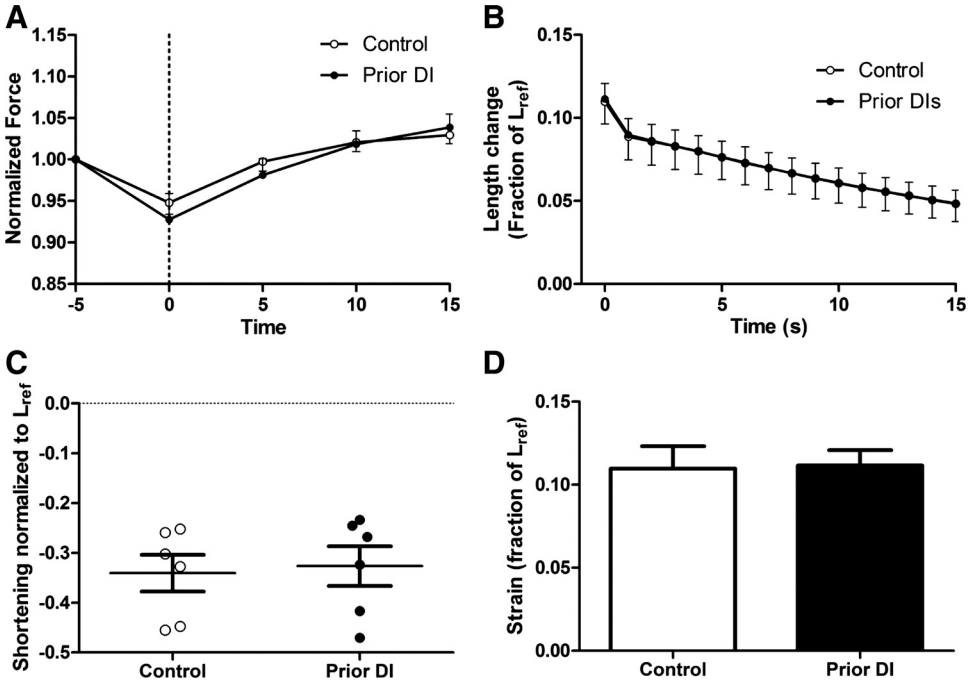

Fig. 6. *A*: force adaptation was induced using 50 nM ACh. Vertical dotted line indicates the first electrical field stimulation (EFS) after ACh administration. Only EFS-induced force is shown. *B*: time course of reshortening following a third DI maneuver in tissues adapted to 50 nM ACh. *C*: maximal shortening preforce controlled DI. *D*: peak strain of tissue in response to a third DI maneuver in tissues adapted to 50 nM ACh. Values are means ± SE.

central question is how many of these can be reopened by a DI, whether control or with prior DIs. Imposing a DI on this challenged lung moves some airways from the closed population to the open one; critically, the number of these reopened airways depends on the ASM force-length dynamics, and it is the alteration of these dynamics by prior DIs that allows additional reopening. In an FEV_1 DI without prior DIs, 254 of those 9,305 closed airways reopen (2.7%). However, in the brochoprotective case with prior DIs, 1,584 reopen (17.0%). This process is illustrated graphically in Fig. 8, which shows the bimodal distribution of open and closed airways in the challenged lung (solid black line), the change in this distribution due to a DI (without prior DIs) as the blue area, and the additional change due to a DI when prior DIs are present as the green area. In terms of resistance at 1 Hz, the FEV_1 DI alone results in a 12.2% decrease relative to baseline, while adding prior DIs resulted in a 43.4% decrease. Clearly the prior DIs lead to a significant increase in the number of reopened airways, as represented by the decrease in the closed population and matching increase in the open population. These data are computed for typical parameter values, but the results are qualitatively the same within a reasonable range of parameter values; for further details, please see the APPENDIX.

Table 1. *Resistance to airflow modeled in a single airway*

Condition	Ratio of Radius (Prior DIs/Control)	Resistance, Pa·s·mm^{-3}	% Change
L_{ref}	1.11 ± 0.02	1.70 ± 0.12	−33.3 ± 4.73
70% L_{ref}	1.01 ± 0.03	2.59 ± 0.35	1.48 ± 13.7
130% L_{ref}	1.04 ± 0.04	2.25 ± 0.32	−11.7 ± 12.6
Force adapted	1.05 ± 0.08	2.85 ± 0.91	11.9 ± 35.6

Values are means ± SE. L_{ref}, reference length. Note: The resistance listed is the minimal resistance achieved during the stretch induced by the third deep inspiration (DI) maneuver in cases where the prior DIs were applied. Percent change is calculated from the difference in the minimal resistance achieved during the stretch induced by the third DI maneuver in between conditions without vs. with prior DIs.

DISCUSSION

The purpose of this study was to test whether intrinsic properties of ASM contribute to, or are the cause of, the bronchoprotective effect of DIs seen in nonasthmatic subjects. We showed that prior DIs have no effect on the level of shortening achieved by the tissues in response to ACh, which is in line with in vivo results showing that prior DIs do not affect airway narrowing (measured by airway conductance, partial maximal expiratory flows, and FEV_1/forced vital capacity) until a subsequent DI is taken (11, 15). Our results also indicate that prior DIs increase the compliance of ACh-shortened ASM strips in response to a subsequent DI-like maneuver

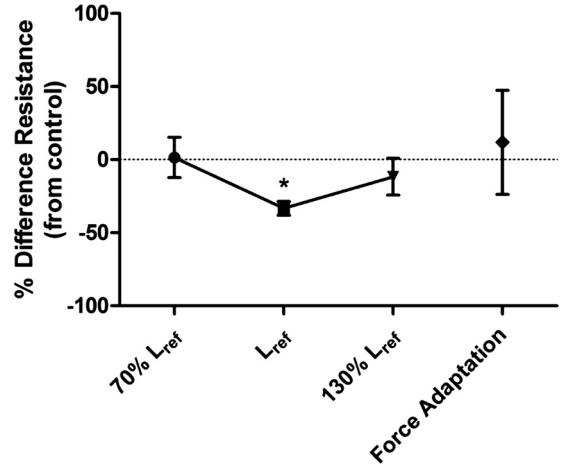

Fig. 7. Change in resistance to airflow caused by prior DIs in each condition. Values are means ± SE. *$P < 0.05$ vs. control, paired Student's *t*-test.

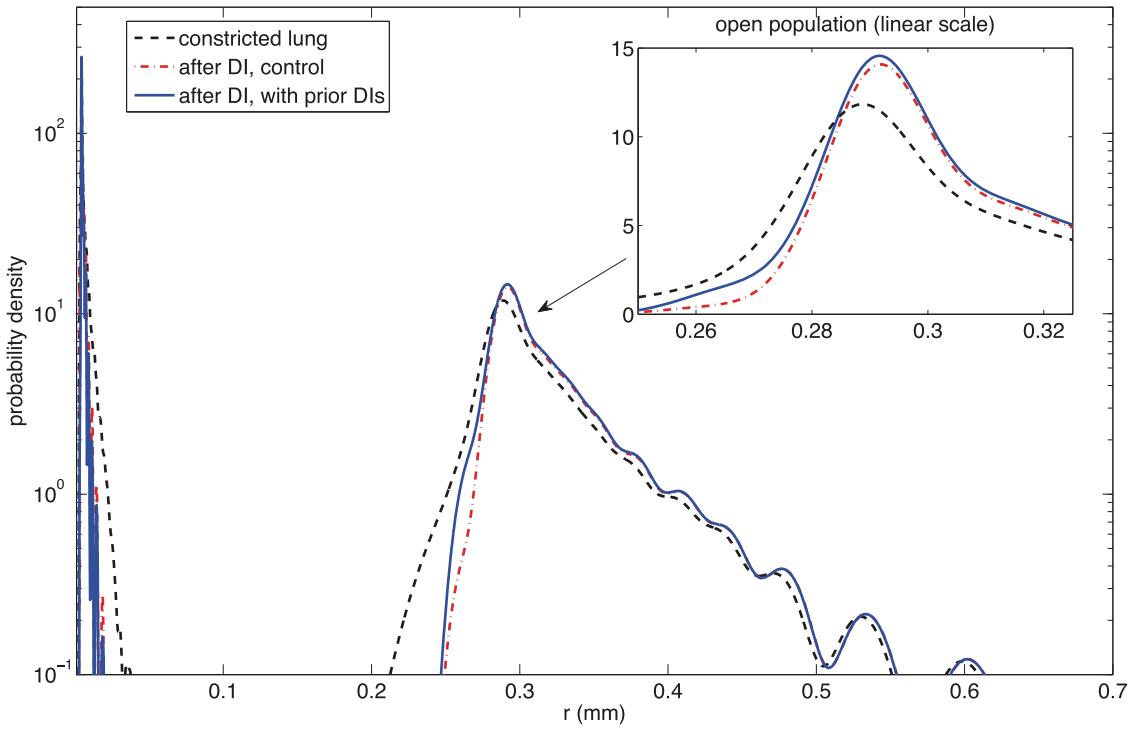

Fig. 8. Distributions of airway radii in challenged lung, with and without DIs. The dashed black curve gives the bimodal distribution of airway radii after agonist challenge, with a population of closed airways near zero radius, and a population of open airways. Note the log scale on the vertical axis, used to visualize both modes. The *inset* figure gives detail of the open population on a linear scale. Imposing a DI on this challenged lung reopens some closed airways, with the new distribution given as a dashed red line: some airways move from the closed population to the open population. Similarly, the solid blue line shows the change in the distribution which occurs from a DI which is after prior DIs (bronchoprotective). In this case, a significant number of additional airways are transferred from the closed population (left peak) to the open population (right peak), and we propose that it is this additional reopening that is responsible for the improvement in lung function from bronchoprotective DIs. For details of the calculation of distributions, please see the APPENDIX.

(i.e., a sudden increase in distending stress). However, the additional increase in ASM elongation engendered by the prior DIs is relatively small and is unlikely to be the sole mechanism for the bronchoprotective effect seen in nonasthmatic subjects. This suggests that other factors are important in determining the extent by which prior DIs protect against a subsequent decrease in FEV_1 elicited by an inhaled challenge with a spasmogen. This point will be addressed later from a different perspective with the help of a mathematical model that simulates the behavior of a heterogeneous population of airways rather than assuming the homogeneous behavior of a "typical" airway.

The results of a number of ex vivo studies designed to investigate how DIs play a role in the dilation of constricted airways (22, 33, 38) or ASM strips (19, 43, 49) have shown that activated ASM is difficult to stretch with simulated DIs. However, the mechanisms of DI-induced bronchodilation and bronchoprotection are likely to be different. DI-induced bronchoprotection involves application of strain to airways and ASM before a constricting stimulus (55). Based on the effects of prior length oscillations on subsequent ASM force generation (19, 53, 59), it was initially hypothesized that DIs might result in changes in the contractile or cytoskeletal apparatus of ASM, which decrease its contractile capacity and thus explain the protective effect of DI. However, the study from Crimi and coworkers (15) showed that prior DIs did not affect the magnitude of subsequent airway narrowing when a surrogate of airway narrowing that did not require a DI was employed. Only when FEV_1 was used as a surrogate of airway narrowing was a significant effect of prior DIs apparent. These in vivo results suggest that the beneficial effects of prior DIs are mediated by improving the effectiveness of the postchallenge DI. Our results support this conclusion in that, in general, ex vivo protocols that included simulated DIs before the administration of ACh resulted in greater effectiveness of the subsequent DI maneuver with respect to its ability to strain the ASM strip. However, the effects are relatively small and by themselves are unlikely to explain the rather substantial protective effect of DIs on the decline in FEV_1 when they preceded the MCh challenge. For example, Kapsali et al. (26) showed that the reduction in FEV_1 of nonasthmatic subjects was blunted by over 80% with prior DIs. Malmberg et al. (36) showed a similar reduction. There is the possibility that in vivo release of mediators, such as nitric oxide or prostaglandin E_2, upon ASM stretch may contribute to the protective and dilatory responses of DIs by actively relaxing the ASM (10, 14, 45). A loss of these mediators in asthma could contribute to the loss of bronchoprotective DIs that is characteristic of the disorder.

The results of Chapman et al. (11) suggest that the salutatory effects of prior DIs are in enabling more effective opening of closed airways by the postchallenge FEV_1-related DI. How could prior DIs affect subsequent airway opening? Besides an effect on the compliance of the ASM, prior DIs could influence the generation of an effective transmural pressure and/or could influence the surface active properties of the airway lining liquid to decrease the opening pressures of closed airways.

Alternatively, the small changes in ASM relengthening we observed could be enough to explain larger differences in the ability to recruit closed airways. Our computational model suggests that the relatively modest differences in ASM response due to prior DIs could, nonetheless, account for a significant bronchoprotective effect by allowing additional reopening of closed airways during the postchallenge DI. This mechanism amplifies the effect of relatively small changes in ASM behavior by way of two sources of nonlinearity: the highly compliant small airways, and the nonlinearity of airflow with respect to airway luminal radius. This amplification mechanism offers one solution to the puzzle posed by the significant bronchoprotective effect seen in vivo, in contrast with the limited influence of simulated DIs in both intact airways (22, 30, 31, 33, 38) and ASM strips (44). Thus it could be that, for a typical airway, a DI does very little, but, by reopening some closed airways, significant changes in lung function are possible.

Wong and colleagues (61) studied mice in an attempt to explain the mechanism for DI-induced bronchoprotection. Paradoxically, they found that prior DIs increased measures of airway narrowing (and the heterogeneity of narrowing), which was consistent with previous study on excised porcine bronchial segments (39). However, like the human in vivo studies, Wong and colleagues showed that a subsequent DI was more effective in dilating airways as assessed by a superior beneficial effect on pulmonary resistance measured using a forced oscillation technique. They also attempted to measure postchallenge airway distensibility by examining the relationship between airway conductance and inflation pressure. Although DIs increased the compliance of the airways prechallenge, there was no difference in distensibility postchallenge with vs. without prior DIs protocols. They concluded that increased compliance of the airway wall (or ASM) is unable to explain the beneficial protective effect of DIs. Like other investigators, they invoked the possible effect on surface tension and thus airway opening pressures (61).

In addition to studying the bronchoprotective effect of prior "DIs" on ASM shortening and relengthening under "normal" conditions (L_{ref} and no tone), we investigated how changes in ASM resting length (length adaptation) and baseline tone (force adaptation) affect ex vivo "bronchoprotection". Length adaptation is a term given to the smooth muscle's ability to maintain contractile capacity over a wide range of lengths (59), and it has been proposed that the phenomenon may contribute to AHR by allowing a chronically narrowed airway to narrow further (7). Force adaptation is a smooth muscle process by which, in the presence of tone, the total force-generating capacity of ASM increases over time. It has been speculated that, in asthma, the constant presence of inflammatory and contractile mediators results in force adaptation (5, 6).

Interestingly, we found that both types of adaptation, to a shorter length and baseline tone, abolished the beneficial effects of prior "DIs". This could be, in part, due to an increased stiffness of ASM at shorter lengths (8) or upon activation (23), thereby limiting either the strain in response to a given stress or the maximal ASM elongation achieved by the simulated DI. This supports the concept that these phenotypic changes, if present in asthmatic subjects, could contribute to the relative ineffectiveness of DI-induced bronchoprotection in asthma. However, adaptation of ASM to a longer length, which would be expected to have the opposite effect, did not enhance the effectiveness of prior "DIs"; in fact, the protective effect of prior "DIs" was marginal after length adaptation to a longer length. This is likely due to an underestimation of the required stretch for the third DI. Since the tissues were adapted to shorter or longer lengths, we would need to adjust the force applied to the muscle to keep a constant pressure amplitude at the shorter or longer lengths (LaPlace's law: tension = pressure $\times$ radius). The problem is that this adjustment is not as simple as increasing the amplitude by 30%, as in the case of tissues adapted to longer lengths. As a result, the amplitude we applied could underestimate the real amplitude that needs to be applied to achieve a stretch equivalent to 25 cmH_2O. This would mean that the marginal protective observed may, in fact, be as large as the tissue at L_{ref}, and that tissues adapted to longer lengths would also benefit from the bronchoprotective effect of DIs. In the case of adaptation to a shorter length, our applied distending force would be overestimating the required stretch, and we still did not see any protection afforded by the DIs. Alternatively, the fixed oscillating strain that was used to simulate prior DIs (which was set to 25% of L_{ref}) represents a smaller relative length change for a muscle adapted to an elongated length, which may explain the attenuated effect of prior DIs on the compliance of ACh-shortened ASM at 130% L_{ref}.

Loss of the bronchoprotective effect of DIs is one of the most consistent markers of asthma. In a recent ex vivo study, the only phenotypic difference in tracheal smooth muscle mechanics between asthmatic and nonasthmatic tissues was deficient force attenuation in response to a series of simulated DIs (12). The results of that study suggest that there is an intrinsic difference in the response to oscillating strain in asthmatic ASM, a difference that could contribute to AHR. It is well known that a decline in contractile capacity is proportional to the magnitude of the strain applied to the ASM (3, 33, 40, 44, 58), and that this occurs regardless of asthmatic status (38). A stiffer airway wall in asthmatic subjects (9, 25, 48) would reduce the strain caused by breathing maneuvers and could be a cause for the loss in the bronchoprotective effect of DIs. There are a host of cytoskeletal proteins that are important in determining the ASM response to DIs, including the focal adhesion proteins vinculin and paxillin, the actin stress fiber protein zyxin (50), and the actin binding proteins actinin and filamin. The role of cytoskeletal proteins in the response to DIs is an overlooked area of research, and more work needs to be done to characterize their role in the active cytoskeletal reorganization that is likely taking place during DIs. Overexpression of some cytoskeletal proteins may enhance the ability of the cytoskeletal network to tolerate or recover from strain caused by DIs in asthmatic subjects and potentially could attenuate the increased compliance in response to the protective DIs. In addition, work by Laube et al. (32) and Lippmann (34) has shown that, while aerosol distribution in the lung is homogenous in nonasthmatic subjects, the distribution is heterogeneous in asthmatic subjects and concentrated in more central airways. However, the model incorporates heterogeneity in the distribution of isometric tensions, which could be the result of heterogeneous distribution of the spasmogen.

The whole lung computational model is designed specifically to test the extent to which alterations in ASM behavior, such as that caused by bronchoprotective DIs, modulate the

reopening of closed airways during DI. The model employs as its key elements the Lambert model for the airway wall (29) and the Lai-Fook model for parenchymal tethering (18) for individual airways in the bronchial tree and thus bears a strong resemblance to several previous models (28, 46). The central differences are *1*) we take the ASM force-length behavior directly from the experimental data for this particular protocol, rather than using a more general representation, and *2*) we assume a bimodal distribution of airway radii in the challenged lung by fiat, without reference to a specific mechanism for its formation. Thus the model is narrowly defined for addressing only the central question we consider here.

Another of the potential limitations of this study is the use of tracheal smooth muscle strips to test the bronchoprotective effect of DIs, which would normally have their major effect in smaller bronchi and bronchioles. However, the purpose of this study was to test the intrinsic response of ASM to prior DIs. In that respect, tracheal smooth muscle is a good model. A limitation of the apparatus used to conduct this study is that it requires that the strip length is returned to resting length after the initial DIs rather than letting it to the increased length (immediately post-DI) as may be occurring in vivo. Thus the conclusions of this paper need to be validated using a different preparation, such as precision-cut lung slices. Work using precision-cut lung slices may also provide a better understanding on how parenchymal tethering plays a role in the protective effect of DIs. Again, the results we present here show a small, but significant, increase in muscle compliance following prior DIs, and it is only in the context of the whole lung that these small changes become physiologically significant as predicted by our model. Future work should be focused on determining what are the main contributors to the bronchoprotective effect of DI in the lung and how they work in concert with ASM to protect the airways of nonasthmatic subjects from constriction.

Conclusion. We conclude that prior DIs confer bronchoprotection by modestly increasing the compliance of contracted ASM. In turn, this increased compliance enhances the strain that the airway wall undergoes during a subsequent DI and, concomitantly, potentiates the bronchodilator effect of DI. This explains why the phenomenon only manifests itself with lung function tests that require a DI. This effect is small when looking at the tissue or airway level. However, when considering the lung as a whole, the small increase of ASM compliance could play a large effect on FEV_1 and forced vital capacity measured in patients by reopening a greater number of closed airways. Finally, phenomena such as length and force adaptations may contribute to the lack of effectiveness of DIs in asthma by preventing the increased compliance of ASM that is normally induced by DIs that preceded the bronchoconstriction.

APPENDIX

This appendix describes the details of the whole lung computational model. The purpose of this model is to ascertain how alterations to the ASM force-length behavior caused by prior DIs, as measured in this work, might regulate the reopening of closed airways during a DI. Thus the model begins from a bistable, constricted state, assumed to result from agonist challenge. The existence of such a state is predicated on the work of others who have considered how such a state might form (1, 2, 57). From such a bistable, constricted state, we then examine the reopening that occurs in response to a DI in both the bronchoprotective and control cases.

The airway tree employed in the computational model is derived from Tawhai et al. (56) with large orders extracted from CT imaging and the remainder generated by a computational algorithm. The lung has 30,941 airways, up to Horsfield order 24.

The dynamics of each individual airway are assumed to be

$$\frac{dr}{dt} = \varrho\left[\Phi(r) - r\right] \tag{A1}$$

where r is the luminal radius (16, 17), and ϱ is an arbitrary time constant. The function $\Phi(r)$ describes the steady-state behavior of the airway, due to a combination of the Lambert model for the airway wall (29), the Lai-Fook model for parenchymal tethering (18), and the Laplace law. Thus

$$\Phi(r) = R\left[\mathrm{P}(r)\right] \tag{A2}$$

where R is the Lambert model for the airway radius, and P is transmural pressure, by composition where the airway wall mechanics are given by Lambert model (29) as

$$R(\mathrm{P}) = \begin{cases} \sqrt{R_i^2(1 - \mathrm{P}/\mathrm{P}_1)^{-n_1}}; & P \le 0 \\ \sqrt{r_{i\max}^2 - (r_{i\max}^2 - R_i^2)(1 - \mathrm{P}/\mathrm{P}_2)^{-n_2}}; & P > 0 \end{cases} \tag{A3}$$

and the transmural pressure P is

$$\mathrm{P}(r) = \mathrm{P}_0 - \frac{\kappa(r_{sm}) \times (r_m - r_w)}{r_{sm}} + \tau(r) \tag{A4}$$

where κ is the smooth muscle pressure, r_{sm} is smooth muscle radius, r_m is muscle radius, and r_w is wall radius. The parenchymal tethering $\tau(r)$ is given by Lai-Fook (18) as

$$\tau(r) = 2\mu\left[\left(\frac{R_{ref} - r_i}{R_{ref}}\right) + 1.5\left(\frac{R_{ref} - r_i}{R_{ref}}\right)^2\right] \tag{A5}$$

where μ is the parenchymal shear modulus, R_{ref} is airway reference ratio, and the smooth muscle radius r_{sm} is

$$r_{sm} = (r_w + r_m)/2 \tag{A6}$$

where

$$r_w = R_i\sqrt{(1 + \varepsilon_w)^2 + (r/R_i)^2 - 1} \tag{A7}$$

and

$$r_m = R_i\sqrt{(1 + \varepsilon_w + \varepsilon_m)^2 + (r/R_i)^2 - 1} \tag{A8}$$

where ε_w and ε_m are parameters characterizing the airway wall thickness and smooth muscle layer thickness, respectively. The ASM force-length behavior is captured by the term $\kappa(r_{sm})$ and depends on the smooth muscle length. We fit the experimental data (force-length curves during force-controlled DI, from this paper) as

$$\kappa_\mu = \hat{\kappa} \times \left(1 - p_1\sqrt{1 - L_0} + p_1\sqrt{L - L_0}\right) \tag{A9}$$

in the stretching phase, and

$$\kappa_d = \hat{\kappa} \times \left(p_1\sqrt{1 - L_0} + p_1\sqrt{\hat{L} - L_0} + p_2\sqrt{\hat{L} - L}\right) \tag{A10}$$

when reshortening. Here $L = 2\pi r_{sm}$ and is normalized to L_{ref}, $\hat{L}$ is the maximum length for each airway during the maneuver, κ_u and κ_d are the effective ASM pressures during stretching and reshortening, respectively, $\hat{\kappa}$ is the reference ASM pressure, and p_1 and p_2 are parameters describing the ASM dynamics.

The agonist challenged lung state is determined by assuming that the $\hat{\kappa}$ are drawn from a normal distribution with prescribed coefficient of variation (CV). The mean of this distribution is then adjusted to reach the target respiratory resistance (5 cmH_2O at 1 Hz). If the resulting ASM tension for an individual airway lies in the region with

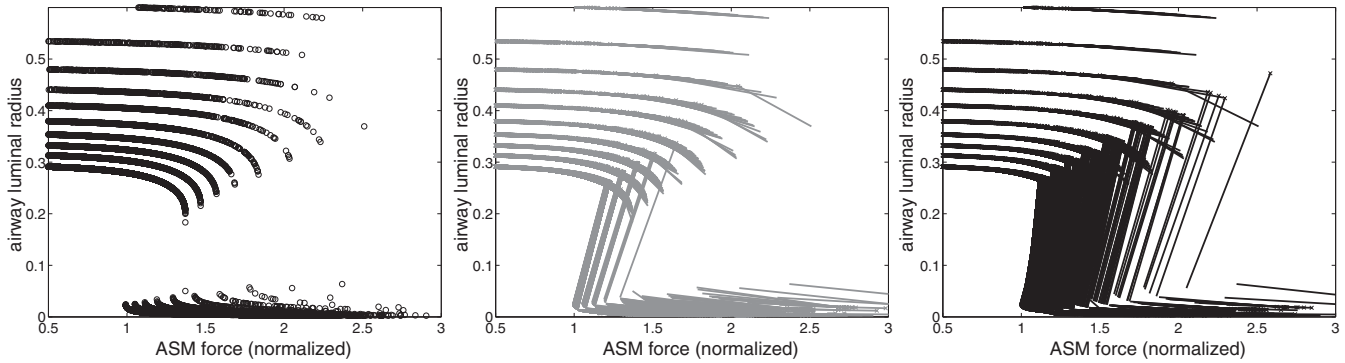

Fig. A1. Airway smooth muscle (ASM) force and airway radii for the small airways. The three panels illustrate three states of the lung. *Left*: the challenged/constricted lung, with a clear bimodal distribution (with respect to radii). *Center*: the response to DI (without prior DIs), with a number of airways being reopened, indicated by the gray lines, taking a previously closed airway into an open position. *Right*: the effect of a DI with prior DIs; here, many more airways are reopened, primarily on account of the altered rate of force increase with stretch, due to altered ASM dynamics. The striations in each figure are a result of the discrete families of airways classified by Horsfield order.

both open and closed branches, a branch is selected at random with equal probability. Simulations with varied CV were also carried out to test the effects of this parameter (see below).

DIs were simulated by making the parameters P_0 and μ time dependent, with a sinusoidal deep breath of duration 8 s and depth 30 cmH_2O.

Individual airway radius and ASM force from the simulations is shown in Fig. A1; these correspond to the distributions shown in Fig. 8, but now give individual force-radius points for each airway, rather than distributions. The *left* panel shows the small airways in the challenged state, with a clear bimodal pattern. The *center* panel shows the changes due to a DI, without prior DIs (control), with the gray lines showing the overall change for each airway from the beginning of the DI to the end, and the gray crosses the final distribution after the end of the DI. Thus lines crossing from the closed population to the open population are the reopening airways. The *right* panel gives the same information in black for the DI with prior DIs (bronchoprotective). Clearly there is additional reopening, and the mechanism for this is the response of the ASM to the DI-induced stretch, specifically, the extent to which airway dilation increases ASM force, as represented by the slope of the response to DI in the force-radius plane. If the slope is steeper (e.g., the ASM force at the end of the DI is lower), then a larger fraction of the airways from the closed population reach the stable, open branch and stays there (hence that airway has reopened).

Respiratory resistance is calculated by a circuit analog model (13, 35). Note that we use resistance because of challenges in simulating FEV_1 directly; however, the inclusion of the FEV_1-like DI immediately before resistance measurement allows us to capture the crucial response to this maneuver.

Sensitivity analysis with respect to both the CV of ASM force and the parenchymal modulus μ was carried out; results presented are typical for large areas of parameter space. The quantitative results given are computed for a 50% CV of ASM force, although sensitivity analysis showed broadly similar results for coefficients of variation ranging from 10 to 100%.

The radius distributions shown in the paper have been estimated from the samples by kernel density estimation, using MATLAB's built-in ksdensity.

Reference radii are taken to be $r_{ref} = R(P_{ref})$. Order-dependent parameters are taken from Politi et al. (46), and the rest are given in Table A1.

Table A1. *Model parameters*

Parameter	Value
P_0	25 cm H_2O
μ	10 cm H_2O
P_{ref}	10 cm H_2O
L_0	0.9
p_1 (control)	4.1
p_2 (control)	−5.9
p_1 (prior DIs)	3.4
p_2 (prior DIs)	−5.3
ϱ	2 (1/s)

P_0, basal pressure; μ, parenchymal shear modulus; P_{ref}, reference transmural pressure; L_0, reference airway smooth muscle length; p_1 and p_2, parameters describing the airway smooth muscle dynamics; ϱ, arbitrary time constant.

ACKNOWLEDGMENTS

The authors acknowledge Dennis Solomon for technical help with tissue dissection and Pitt Meadow Valley Meats for supplying the fresh sheep trachea in kind.

GRANTS

This work was supported by operating grants from Canadian Institutes of Health Research (CIHR) (MOP-13271, MOP-37924) and Discovery Grant from the Natural Sciences and Engineering Research Council of Canada. C. D. Pascoe is supported by an affiliated fellowship from the University of British Columbia.

DISCLOSURES

No conflicts of interest, financial or otherwise, are declared by the author(s).

AUTHOR CONTRIBUTIONS

Author contributions: C.D.P., G.M.D., C.Y.S., and P.D.P. conception and design of research; C.D.P. performed experiments; C.D.P., G.M.D., C.Y.S., and P.D.P. analyzed data; C.D.P., G.M.D., C.Y.S., and P.D.P. interpreted results of experiments; C.D.P. and G.M.D. prepared figures; C.D.P. drafted manuscript; C.D.P., G.M.D., Y.B., C.Y.S., and P.D.P. edited and revised manuscript; C.D.P., G.M.D., Y.B., C.Y.S., and P.D.P. approved final version of manuscript.

REFERENCES

1. **Affonce DA, Lutchen KR.** New perspectives on the mechanical basis for airway hyperreactivity and airway hypersensitivity in asthma. *J Appl Physiol* 101: 1710–1719, 2006.
2. **Anafi RC, Wilson TA.** Airway stability and heterogeneity in the constricted lung. *J Appl Physiol* 91: 1185–1192, 2001.
3. **Ansell TK, McFawn PK, Mitchell HW, Noble PB.** Bronchodilatory response to deep inspiration in bronchial segments: the effects of stress vs. strain. *J Appl Physiol* 115: 505–13, 2013.
4. **Bai TR, Bates JHT, Brusasco V, Camoretti-Mercado B, Chitano P, Deng LH, Dowell M, Fabry B, Ford LE, Fredberg JJ, Gerthoffer WT, Gilbert SH, Gunst SJ, Hai CM, Halayko AJ, Hirst SJ, James AL, Janssen LJ, Jones KA, King GG, Lakser OJ, Lambert RK, Lauzon**

AM, Lutchen KR, Maksym GN, Meiss RA, Mijailovich SM, Mitchell HW, Mitchell RW, Mitzner W, Murphy TM, Paré PD, Schellenberg RR, Seow CY, Sieck GC, Smith PG, Smolensky AV, Solway J, Stephens NL, Stewart AG, Tang DD, Wang L. On the terminology for describing the length-force relationship and its changes in airway smooth muscle. *J Appl Physiol* 97: 2029–2034, 2004.

5. **Bossé Y, Chin LY, Paré PD, Seow CY.** Adaptation of airway smooth muscle to basal tone: relevance to airway hyperresponsiveness. *Am J Respir Cell Mol Biol* 40: 13–18, 2009.
6. **Bosse Y, Pare PD.** Histamine and endogenously produced spasmogenic prostaglandins increase the strength of airway smooth muscle (Abstract). *J Allergy Clin Immunol* 129: 52, 2012.
7. **Bosse Y, Sobieszek A, Pare PD, Seow CY.** Length adaptation of airway smooth muscle. *Proc Am Thorac Soc* 5: 62–67, 2008.
8. **Bossé Y, Solomon D, Chin LYM, Lian K, Paré PD, Seow CY.** Increase in passive stiffness at reduced airway smooth muscle length: potential impact on airway responsiveness. *Am J Physiol Lung Cell Mol Physiol* 298: L277–L287, 2010.
9. **Brown NJ, Salome CM, Berend N, Thorpe CW, King GG.** Airway distensibility in adults with asthma and healthy adults, measured by forced oscillation technique. *Am J Respir Crit Care Med* 176: 129–137, 2007.
10. **Brown RH, Mitzner W.** Airway response to deep inspiration: role of nitric oxide. *Eur Respir J* 22: 57–61, 2003.
11. **Chapman DG, Berend N, King GG, McParland BE, Salome CM.** Deep inspirations protect against airway closure in nonasthmatic subjects. *J Appl Physiol* 107: 564–569, 2009.
12. **Chin LY, Bosse Y, Pascoe CD, Hackett TL, Seow CY, Pare PD.** Mechanical properties of asthmatic airway smooth muscle. *Eur Respir J* 40: 45–54, 2012.
13. **Chiu WWC.** *Multi-scale Models of Respiratory Impedance and Bimodal Ventilation*. Auckland, New Zealand: Bioengineering, University of Auckland, 2011.
14. **Copland IB, Reynaud D, Pace-Asciak C, Post M.** Mechanotransduction of stretch-induced prostanoid release by fetal lung epithelial cells. *Am J Physiol Lung Cell Mol Physiol* 291: L487–L495, 2006.
15. **Crimi E, Pellegrino R, Milanese M, Brusasco V.** Deep breaths, methacholine, and airway narrowing in healthy and mild asthmatic subjects. *J Appl Physiol* 93: 1384–1390, 2002.
16. **Donovan GM, Kritter T.** Spatial pattern formation in the lung. *J Math Biol*. In press.
17. **Donovan GM, Sneyd J, Tawhai MH.** The importance of synergy between deep inspirations and fluidization in reversing airway closure. *PLos One* 7: e48552, 2012.
18. **Lai-Fook SJ.** A continuum mechanics analysis of pulmonary vascular interdependence in isolated dog lobes. *J Appl Physiol* 46: 419–429, 1979.
19. **Fredberg JJ, Inouye D, Miller B, Nathan M, Jafari S, Raboudi SH, Butler JP, Shore SA.** Airway smooth muscle, tidal stretches, and dynamically determined contractile states. *Am J Respir Crit Care Med* 156: 1752–1759, 1997.
20. **Gayrard P, Orehek J, Grimaud C, Charpin J.** Bronchoconstrictor effects of a deep inspiration in patients with asthma. *Am Rev Respir Dis* 111: 433–439, 1975.
21. **Gunst SJ, Wu MF.** Selected Contribution: Plasticity of airway smooth muscle stiffness and extensibility: role of length-adaptive mechanisms. *J Appl Physiol* 90: 741–749, 2001.
22. **Harvey BC, Parameswaran H, Lutchen KR.** Can tidal breathing with deep inspirations of intact airways create sustained bronchoprotection or bronchodilation? *J Appl Physiol* 115: 436–445, 2013.
23. **Hubmayr RD, Shore SA, Fredberg JJ, Planus E, Panettieri RA, Moller W, Heyder J, Wang N.** Pharmacological activation changes stiffness of cultured human airway smooth muscle cells. *Am J Physiol Cell Physiol* 271: C1660–C1668, 1996.
24. **James AL, Pare PD, Hogg JC.** The mechanics of airway narrowing in asthma. *Am Rev Respir Dis* 139: 242–246, 1989.
25. **Johns DP, Wilson J, Harding R, Walters EH.** Airway distensibility in healthy and asthmatic subjects: effect of lung volume history. *J Appl Physiol* 88: 1413–1420, 2000.
26. **Kapsali T, Permutt S, Laube B, Scichilone N, Togias A.** Potent bronchoprotective effect of deep inspiration and its absence in asthma. *J Appl Physiol* 89: 711–720, 2000.
27. **Kuwano K, Bosken CH, Pare PD, Bai TR, Wiggs BR, Hogg JC.** Small airways dimensions in asthma and in chronic obstructive pulmonary disease. *Am Rev Respir Dis* 148: 1220–1225, 1993.
28. **Lambert RK, Wilson TA.** Smooth muscle dynamics and maximal expiratory flow in asthma. *J Appl Physiol* 99: 1885–1890, 2005.
29. **Lambert RK, Wilson TA, Hyatt RE, Rodarte JR.** A computational model for expiratory flow. *J Appl Physiol* 52: 44–56, 1982.
30. **LaPrad AS, Szabo TL, Suki B, Lutchen KR.** Tidal stretches do not modulate responsiveness of intact airways in vitro. *J Appl Physiol* 109: 295–304, 2010.
31. **LaPrad AS, West AR, Noble PB, Lutchen KR, Mitchell HW.** Maintenance of airway caliber in isolated airways by deep inspiration and tidal strains. *J Appl Physiol* 105: 479–485, 2008.
32. **Laube BL, Norman PS, Adams GK III.** The effect of aerosol distribution on airway responsiveness to inhaled methacholine in patients with asthma. *J Allergy Clin Immunol* 89: 510–518, 1992.
33. **Lavoie TL, Krishnan R, Siegel HR, Maston ED, Fredberg JJ, Solway J, Dowell ML.** Dilatation of the constricted human airway by tidal expansion of lung parenchyma. *Am J Respir Crit Care Med* 186: 225–232, 2012.
34. **Lippmann M.** Regional deposition of particles in the human respiratory tract. In: *Comprehensive Physiology*. New York: Wiley, 2011, Suppl. 26, p. 213–232. (Online) http://onlinelibrary.wiley.com/doi/10.1002/cphy.cp090114/full [29 Aug 2014].
35. **Lutchen KR, Costa KD.** Physiological interpretations based on lumped element models fit to respiratory impedance data: use of forward-inverse modeling. *IEEE Trans Biomed Eng* 37: 1076–1086, 1990.
36. **Malmberg P, Larsson K, Sundblad BM, Zhiping W.** Importance of the time interval between FEV_1 measurements in a methacholine provocation test. *Eur Respir J* 6: 680–686, 1993.
37. **Naghshin J, Wang L, Pare PD, Seow CY.** Adaptation to chronic length change in explanted airway smooth muscle. *J Appl Physiol* 95: 448–453; discussion 435, 2003.
38. **Noble PB, Jones RL, Cairncross A, Elliot JG, Mitchell HW, James AL, McFawn PK.** Airway narrowing and bronchodilation to deep inspiration in bronchial segments from subjects with and without reported asthma. *J Appl Physiol* 114: 1460–1471, 2013.
39. **Noble PB, McFawn PK, Mitchell HW.** Intraluminal pressure oscillation enhances subsequent airway contraction in isolated bronchial segments. *J Appl Physiol* 96: 1161–1165, 2004.
40. **Noble PB, McFawn PK, Mitchell HW.** Responsiveness of the isolated airway during simulated deep inspirations: effect of airway smooth muscle stiffness and strain. *J Appl Physiol* 103: 787–795, 2007.
41. **Oliver MN, Fabry B, Marinkovic A, Mijailovich SM, Butler JP, Fredberg JJ.** Airway hyperresponsiveness, remodeling, and smooth muscle mass: right answer, wrong reason? *Am J Respir Cell Mol Biol* 37: 264–272, 2007.
42. **Orehek J, Charpin D, Velardocchio JM, Grimaud C.** Bronchomotor effect of bronchoconstriction-induced deep inspirations in asthmatics. *Am Rev Respir Dis* 121: 297–305, 1980.
43. **Pascoe CD, Jiao Y, Seow CY, Pare PD, Bosse Y.** Force oscillations simulating breathing maneuvers do not prevent force adaptation. *Am J Respir Cell Mol Biol* 47: 44–49, 2012.
44. **Pascoe CD, Seow CY, Paré PD, Bossé Y.** Decrease of airway smooth muscle contractility induced by simulated breathing maneuvers is not simply proportional to strain. *J Appl Physiol (1985)* 114: 335–343, 2013.
45. **Piper P, Vane J.** The release of prostaglandins from lung and other tissues. *Ann N Y Acad Sci* 180: 363–385, 1971.
46. **Politi AZ, Donovan GM, Tawhai MH, Sanderson MJ, Lauzon AM, Bates JHT, Sneyd J.** A multiscale, spatially distributed model of asthmatic airway hyper-responsiveness. *J Theor Biol* 266: 614–624, 2010.
47. **Pratusevich VR, Seow CY, Ford LE.** Plasticity in canine airway smooth muscle. *J Gen Physiol* 105: 73–94, 1995.
48. **Pyrgos G, Scichilone N, Togias A, Brown RH, Pyrgos G, Scichilone N, Togias A, Brown RH.** Bronchodilation response to deep inspirations in asthma is dependent on airway distensibility and air trapping. *J Appl Physiol* 110: 472–479, 2011.
49. **Raqeeb A, Solomon D, Paré PD, Seow CY.** Length oscillation mimicking periodic individual deep inspirations during tidal breathing attenuates force recovery and adaptation in airway smooth muscle. *J Appl Physiol* 109: 1476–1482, 2010.

50. **Rosner SR, Blankman E, Jensen CC, Krishnan R, Beckerle MC, Fredberg JJ, Smith M.** Bronchospasm, deep inspirations and the paradoxical role of zyxin (Abstract). *Am J Respir Crit Care Med* 189: A3667, 2014.
51. **Scichilone N, Kapsali T, Permutt S, Togias A.** Deep inspiration-induced bronchoprotection is stronger than bronchodilation. *Am J Respir Crit Care Med* 162: 910–916, 2000.
52. **Scichilone N, Permutt S, Togias A.** The lack of the bronchoprotective and not the bronchodilatory ability of deep inspiration is associated with airway hyperresponsiveness. *Am J Respir Crit Care Med* 163: 413–419, 2001.
53. **Shen X, Wu MF, Tepper RS, Gunst SJ.** Mechanisms for the mechanical response of airway smooth muscle to length oscillation. *J Appl Physiol* 83: 731–738, 1997.
54. **Skloot G, Permutt S, Togias A.** Airway hyperresponsiveness in asthma: a problem of limited smooth muscle relaxation with inspiration. *J Clin Invest* 96: 2393–2403, 1995.
55. **Skloot G, Togias A.** Bronchodilation and bronchoprotection by deep inspiration and their relationship to bronchial hyperresponsiveness. *Clin Rev Allergy Immunol* 24: 55–71, 2003.
56. **Tawhai MH, Nash MP, Hoffman EA.** An imaging-based computational approach to model ventilation distribution and soft-tissue deformation in the ovine lung. *Acad Radiol* 13: 113–120, 2006.
57. **Venegas JG, Winkler T, Musch G, Vidal Melo MF, Layfield D, Tgavalekos N, Fischman AJ, Callahan RJ, Bellani G, Scott Harris R.** Self-organized patchiness in asthma as a prelude to catastrophic shifts. *Nature* 434: 777–782, 2005.
58. **Wang L, Paré PD, Seow CY.** Effects of length oscillation on the subsequent force development in swine tracheal smooth muscle. *J Appl Physiol* 88: 2246–2250, 2000.
59. **Wang L, Paré PD, Seow CY.** Selected Contribution: Effect of chronic passive length change on airway smooth muscle length-tension relationship. *J Appl Physiol* 90: 734–740, 2001.
60. **Wiggs BR, Moreno R, Hogg JC, Hilliam C, Paré PD.** A model of the mechanics of airway narrowing. *J Appl Physiol* 69: 849–860, 1990.
61. **Wong RS, Larcombe AN, Fernandes LB, Zosky GR, Noble PB.** The mechanism of deep inspiration-induced bronchoprotection: evidence from a mouse model. *Eur Respir J* 40: 982–989, 2012.